Continental Shelf Research 31 (2011) S37–S47

Contents lists available at ScienceDirect

Continental Shelf Research

journal homepage: www.elsevier.com/locate/csr

Research papers

The coupling of temporal and spatial variations of chlorophyll a concentration and the East Asian monsoons in the southern Taiwan Strait

Huasheng Hong [a], Xin Liu [a], Kuo-Ping Chiang [b], Bangqin Huang [a,*], Caiyun Zhang [a], Jun Hu [a], Yonghong Li [a]

[a] State Key Laboratory of Marine Environmental Science, Fujian Key Laboratory of Coastal Ecology and Environmental Studies, Xiamen University, 361005 Xiamen, Fujian
[b] Institute of Environmental Biology and Fishery Science, National Taiwan Ocean University, Keelung 202-24, Taiwan

ARTICLE INFO

Article history:
Accepted 26 January 2011
Available online 12 February 2011

Keywords:
Seasonal variations
Chl *a*
Upwelling
Physical–biological coupling
Taiwan Strait

ABSTRACT

The impact of monsoon on the temporal and spatial variations of phytoplankton standing stock (Chl *a*) in the southern Taiwan Strait was studied based on long-term satellite data (1997–2008) and field observations (during 1987–1988 and 2006–2007). During the NorthEast (NE) monsoon, the high Chl *a* was induced by vertical mixing, the Zhejiang–Fujian Coastal Current and upwelling. However, for most of the area, the vertical mixing was the dominant process that enhanced phytoplankton growth. During the SouthWest (SW) monsoon, two low temperature and high Chl *a* areas were observed: one near the Dongshan Island and the other in the southeast edge of the Taiwan Bank. Both of them were identified as the upwelling areas a half century ago. The Dongshan upwelling is mainly caused by the cold waters, which is derived from the famous "East Guangdong upwelling" induced by the SW monsoon. And the latter upwelling is mainly induced by a shallowing of the topography and the Kuroshio intrusion. In the last decades, most of the studies suggested that the Chl *a* during the SW monsoon is higher than that during the NE monsoon, due to the upwelling and cold temperature, respectively. However, some recent studies made contrary conclusion. Using the satellite seasonal climatological Chl *a* data (SeaWiFS and MODIS), we acquired more extensive and long-term records and found a significant difference in the temporal variation patterns of Chl *a* concentrations in the three sub-areas of southern Taiwan Strait. In the coastal area, two Chl *a* peaks were observed, which were due to upwelling during the SW monsoon and Zhejiang–Fujian Coastal Current during the NE monsoon. On the Taiwan Bank, the high Chl *a* occurred throughout the year due to the topographical upwelling all year round. For the shelf break area, a higher Chl *a* was observed during the NE monsoon, which was induced by vertical mixing. For the whole study area, a significant coupling occurred between Chl *a* and wind speed ($r^2=0.23$, $p<0.05$) during the NE monsoon, while it was very weak during the SW monsoon. On the other hand, the mean surface Chl *a* was significantly higher in the NE monsoon (0.69 mg m^{-3}) than in the SW monsoon (0.53 mg m^{-3}). All these results demonstrated that the temporal and spatial variations of phytoplankton standing stock were affected by the East Asia monsoon system in the southern Taiwan Strait.

1. Introduction

The Taiwan Strait is an important channel between the East China Sea and South China Sea, with complex hydrodynamics as shown in Fig. 1. The South China Sea Warm Current extends northeastwards along the continental shelf (Hu et al., 2000). The Kuroshio intrudes into the northern South China Sea year-round though the Luzon Strait (Shaw, 1989, 1991; Jan et al., 1998; Hu et al., 2000). On the near shore side, the Zhejiang–Fujian Coastal Current, characterized by low temperature and nutrient-rich water has significant impacts on the southern Taiwan Strait during the NorthEast (NE) monsoon period (Jan et al., 1998, 2006; Lee et al., 2005).

Similar to the situation in the Arabian Sea, the climate and marine ecosystem of the southern Taiwan Strait is affected by the East Asia Monsoon, with a strong NE monsoon prevails over the Taiwan Strait from October to April, and a weak southwest (SW) monsoon prevails from June to August (Chen et al., 2006). The SW monsoon induces some active upwelling events in the southern Taiwan Strait. The Dongshan upwelling, near Dongshan Island, is the largest and strongest one in the Taiwan Strait which is principally induced by the Ekman transport during the SW

* Corresponding author: Tel.: +86 592 2187783; fax: +86 592 2180655.
E-mail address: bqhuang@xmu.edu.cn (B. Huang).

0278-4343/$ - see front matter © 2011 Elsevier Ltd. All rights reserved.
doi:10.1016/j.csr.2011.02.004

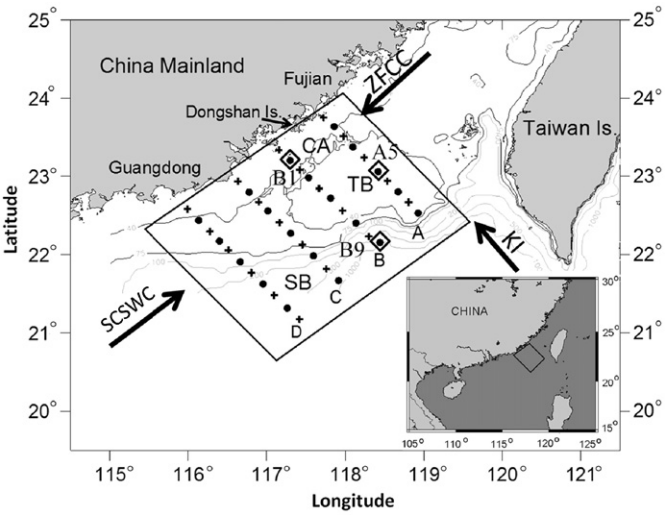

Fig. 1. Sampling stations in the southern Taiwan Strait. Hydrographic stations (+) and physical, chemical and biological stations (●). The three sub-areas were TB, the Taiwan Bank area, was defined as water with depth less than 40 m. CA, the coastal area, was defined as the area with depths less than 75 m but excluding the Taiwan Bank area, and SB, the shelf break area, involved depths greater than 75 m. Three representative stations B1, A5 and B9 are marked as ⋄. ZFCC: Zhejiang–Fujian Coastal Current, KI: Kuroshio Intrusion, SCSWC: South China Sea Warm Current.

monsoon (Tang et al. 2002; Hu et al., 2003). The Taiwan Bank upwelling, in the southern edge of the Taiwan Bank with its banana-like shape, occurs year-round with varying strength and scale. Wind stress, tides, bottom topography and the Kuroshio intrusion are four important influential factors in the formation of this upwelling (Hu et al., 2003). Tang et al. (2002) indicated that these upwelled areas, with its 2–3 °C lower temperature than the non-upwelling area, are consistent with the appearance of a high Chl *a* area during the SW monsoon period. Furthermore, Hu (2009) reveals that diatom dominates the phytoplankton community in coastal upwelling area with 72% in term of total Chl *a*. At the shelf break area, cyanobacteria and prochlorophytes are the main contributors for total Chl *a* (up to 82%). Hu et al. (2003) review the upwelling system in the Taiwan Strait, and indicate that the upwelling is very complicated in this area, especially the Taiwan Bank upwelling. They note that the upwelling is a multi-cell structure in the southern Taiwan Strait, and there are at least three independent upwelling water masses with different physical and chemical characteristics.

Seasonal variation features of Chl *a* in the southern Taiwan Strait have been studied for decades, however, it remains unclear as there are conflicting reports on underlying processes (Hong et al., 1991; Zhang et al., 1997; Wan et al., 2007 and references therein). Most of the studies suggest that the Chl *a* during the SW monsoon is higher than that during the NE monsoon. The results show that the peak of Chl *a* in summer (SW monsoon) is due to nutrient input by upwelling. In the winter (NW monsoon), they suggest that although the Zhejiang–Fujian Coastal Current can provide rich nutrients for phytoplankton growth, low temperature and high turbidity may be limiting factors of phytoplankton growth, especially, in the coastal and estuary areas (Zhang et al., 1997, 2002; Naik and Chen, 2008). However, some studies exhibit the contrary results (Hong et al., 1997; Zhang, 2006b; Wang et al., 2002; Kang, 2009). Due to the influence of the South China Sea and Kuroshio, the phenomenon that temperature limits phytoplankton growth in wintertime cannot happen in the most areas of southern Taiwan Strait (Zhang, 2006b; Kang, 2009). In addition, they suggest that there are different seasonal variation patterns of Chl *a* in the southern Taiwan Strait, compared to the northern Strait. The size-fractioned phytoplankton biomass and productivity are also different between the northern and the southern Taiwan Strait. Nanophytoplankton (3–20 μm) dominated the phytoplankton community in the northern Taiwan Strait while picophytoplankton (0.2–3 μm) dominated in the southern Taiwan Strait (Huang et al., 1999). All these results demonstrate that the phytoplankton community is significantly influenced by biogeochemical processes in the southern Taiwan Strait and the mechanism is totally different between NE monsoon and SW monsoon (Huang et al., 1999; Naik and Chen, 2008).

As monsoon-driven area, the relationship between phytoplankton and temporal monsoon variations in the Arabian Sea has been a subject of interest, and has made significant progress (Schott and McCreary, 2001, and references therein). However, it remains unresolved issue in the southern Taiwan Strait. First, the unstable upwelling event causes the phytoplankton standing stocks to exhibit high temporal and spatial variations in the coastal area during the SW monsoon, and during the NE monsoon, both the nutrient-rich Zhejiang–Fujian Coastal Current water and the vertical mixing can support the high phytoplankton biomass, but low temperature and high turbidity may also limit phytoplankton growth. In addition, few field data were available on the ecological impact of coastal currents and vertical mixing in the wintertime. There may not be a simple description of the temporal variations of Chl *a* based on a couple of cruises in the southern Taiwan Strait (Hong et al., 1991, 1997; Wang et al., 2002; Zheng et al., 2002; Naik and Chen, 2008; Kang, 2009). Second, since the hydrodynamics is complex in the southern Taiwan Strait, the nutrient inputs are different with the different areas (e.g. coast, shelf and Taiwan Bank). Third, few studies have been done on the coupling among phytoplankton standing stock, wind, upwelling, coastal current and vertical mixing in this area, and the relationship between wind speeds and Chl *a* is unclear. Therefore, based on long-term satellite data and field observations in the southern Taiwan Strait, the present study investigates the temporal and spatial variations of Chl *a* and illustrates the different control processes in the three sub-areas of the southern Taiwan Strait.

2. Materials and methods

The study area was in the southern Taiwan Strait as shown in Fig. 1. Four field survey cruises were carried out during December 1987, July 1988, August 2006 and February 2007. A total of 40 sampling stations were located along four cross-shelf transects. Temperature and salinity were recorded with a reversing thermometer and a salinometer during the cruises in 1987–1988 and with a Sea-Bird Conductivity–Temperature–Depth recorder (CTD) during the cruises in 2006–2007. Discrete seawater samples were collected and analyzed for nutrients and Chl *a*. Nutrient analysis was performed on board ship using standard manual spectrophotometric methods (Parsons et al., 1984; Pai et al., 1990a, 1990b), and the detection limits of nitrate, phosphate and silicate were 0.5, 0.1 and 0.5 μmol L^{-1}, respectively. Chl *a* was determined by spectrophotometric analysis during 1987–1988 (Jeffrey and Humphrey, 1975) and fluorescence analysis during 2006–2007 (Parsons et al., 1984). The Chl *a* samples were prepared by filtering 150–300 mL seawater through polycarbonate filter (0.45 μm in pore size), and then the filter was stored at −20 °C until analysis.

The monthly mean wind data were retrieved from Quik Scatterometer (QuikSCAT) observations from August, 1999 to July, 2008. The spatial resolution was 0.25° by 0.25° for QuikSCAT winds. The monthly mean Sea Surface Temperature (SST) data in the southern Taiwan Strait were derived from NOAA AVHRR Pathfinder SST products from January, 1985 to December, 2006, with a spatial resolution of 4 by 4 km. The surface Chl *a* was

derived from Sea-viewing Wide Field-of-view Sensor (SeaWiFS) from December, 1997 to December, 2003, and Moderate Resolution Imaging Spectrometer (MODIS) from January, 2004 to December, 2007, as the data availability permitted. The SeaWiFS daily Level-1A data were obtained from the NASA Distributed Active Archive Center (DAAC). They were processed to Level 2 Chl *a* data products using the SeaWiFS Data Analysis System (SeaDAS4.6) software, and then mapped to a cylindrical equidistant projection at 1 km/pixel resolution. Atmospheric effects were removed with the Gordon and Wang (1994) algorithm to obtain the normalized spectral water-leaving radiance (nLw(λ)), which were then used in the OC4v4 band-ratio algorithm (O'Reilly et al., 2000) to estimate Chl *a*. The daily data were used to generate monthly composite (arithmetic mean) images while discarding suspicious pixels associated with various flags (e.g., cloud/stray light, large solar/sensor angle, high aerosol optical thickness). Daily MODIS/Aqua data covering the study region were processed by the NASA Goddard Space Flight Center (GSFC) using similar atmospheric correction algorithms as for SeaWiFS (Collection 4), but with the OC3 (O'Reilly et al., 2000) bio-optical algorithm.

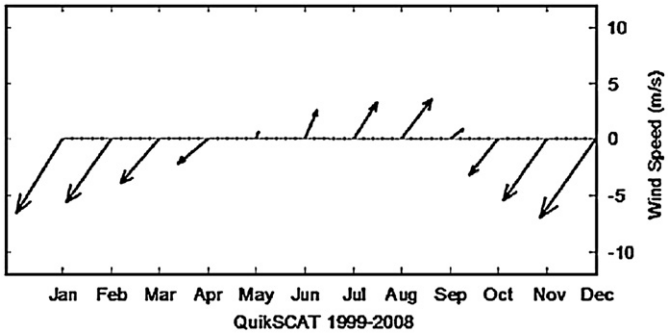

Fig. 2. Climatological (1999–2008) monthly mean QuikSCAT wind speed in the southern Taiwan Strait.

In previous studies (Shang et al., 2004; Zhang et al., 2006a), the distributions of surface Chl *a* in the southern Taiwan Strait that

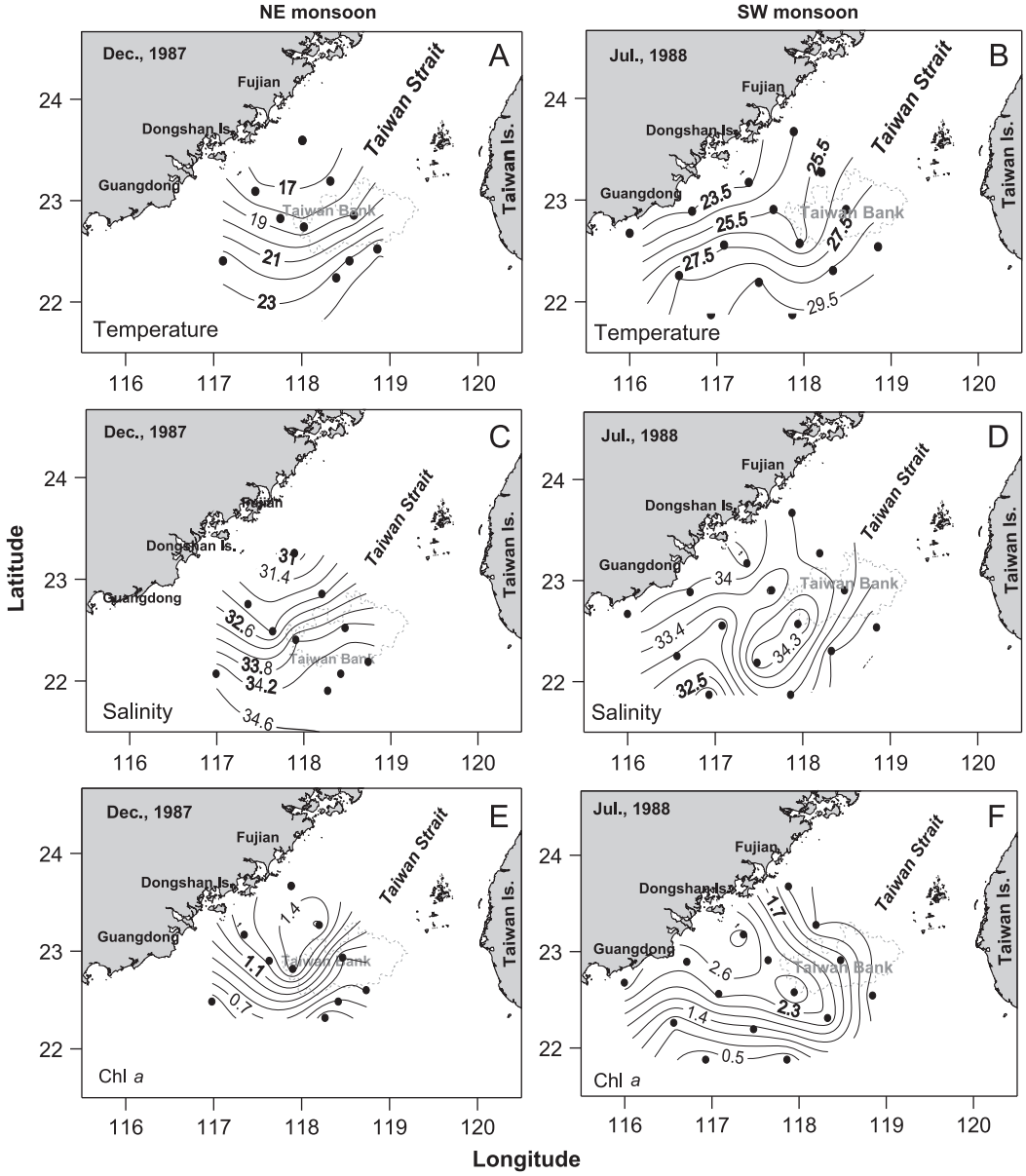

Fig. 3. Horizontal distribution of temperature (A, B), salinity (C, D) and chlorophyll *a* concentration (E, F, the euphotic zone integrated mean value, mg m^{-3}) during the NorthEast (NE) monsoon (left panel) and SouthWest (SW) monsoon (right panel) oceanographic cruises during 1987–1988.

derived from satellite data were found to be consistent with those derived from concurrent field observations. In addition, Zhang et al. (2006a) demonstrated that it would be possible to use MODIS and SeaWiFS together in continuous time series analyses.

For a comparative study among upwelling zones and the surrounding areas, we divided the study area into the three sub-areas (Fig. 1). Within the study area box, the Taiwan Bank area was defined as the area with a depth <40 m. The coastal area was defined as the area with a depth <75 m but excluding the Taiwan Bank area, while the shelf break area with a depth ≥ 75 m. Based on wind data (Fig. 2), we defined the typical NE and SW monsoon seasons as December–February and June–August, respectively. We did calculations on long-term mean Chl *a* and SST based on these three sub-areas and periods. A one-way ANOVA and paired sample test was used for statistical analysis (SPSS V16.0). The significance level was set at $p<0.05$. ANOVA results were compared using the least significant difference (LSD) method.

3. Results

3.1. The climatological monthly mean wind velocity

The climatological (1999–2008) monthly mean QuikSCAT wind velocity showed the typical features of the East Asian monsoon in the southern Taiwan Strait (Fig. 2). A maximum wind speed of 9 m s^{-1} was observed in December during the strong NE monsoon period, and another peak (4.7 m s^{-1}) was noted in August during the SW monsoon. Therefore, it was easily divided into two phases: the NE monsoon and the SW monsoon. The NE monsoon (dry season) was from October to April. In comparison with the NE monsoon, the force of the SW monsoon (wet season) was smaller. It began in June and became weaker in September, with the maximum in July and August.

3.2. Field observations

During the NE monsoon period (December, 1987), the high Chl *a* of the southern Taiwan Strait was induced by the high nutrient Zhejiang–Fujian Coastal Current water and strong vertical mixing. The Zhejiang–Fujian Coastal Current, characterized by low temperature (<17 °C), low salinity (<32) and high Chl *a* (the average integrated Chl $a>1.4$ mg m^{-3}), flowed southward into the southern Taiwan Strait along the coast of mainland China (Fig. 3A, C and E). High temperature (>22 °C), high salinity (>34.25) and oligotrophic water with low Chl *a* water (<0.7 mg m^{-3}), which are South China Sea and intrude Kuroshio water, occupied the shelf break area. The Chl *a* on the north coast was higher than 1.45 mg m^{-3}, and gradually decreased to the south and shelf break area (0.5 mg m^{-3}). However, the water column showed a homogenous vertical distribution along the transect during NE monsoon (Fig. 4A, C and E). There were very few differences of temperature, salinity and Chl *a* between the

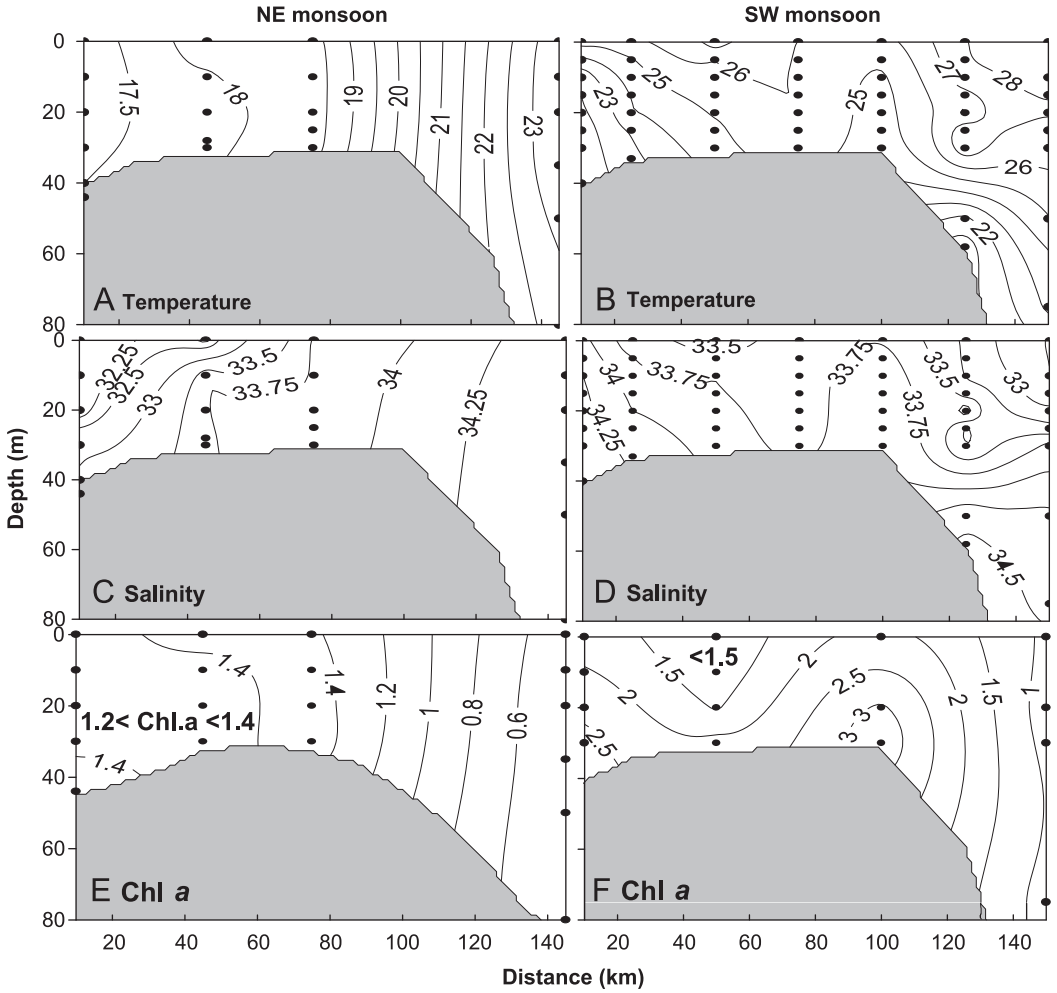

Fig. 4. Variations of temperature (A, B), salinity (C, D) and chlorophyll *a* (E, F) along Transect B in the southern Taiwan Strait during the NorthEast (NE) monsoon (left panel) and SouthWest (SW) monsoon (right panel) oceanographic cruises during December 1987, and July 1988.

surface and bottom layers, except Zhejiang–Fujian Coastal Current water with the low salinity in surface layer of the coastal stations (Fig. 4C, <20 m).

Two areas of upwelled waters, as indicated by low temperature (<23.5 °C) and high salinity (>34), appeared in the coastal and Taiwan Bank areas during the SW monsoon period (Fig. 3B, D and F). The former was near Dongshan Island, namely the Dongshan upwelling. The latter was the Taiwan Bank upwelling, which was located to the southwest of the Taiwan Bank. High concentrations of Chl *a* were observed in the center of both the Dongshan upwelling (2.9 mg m^{-3}) and the Taiwan Bank upwelling (2.75 mg m^{-3}). A similar distribution pattern also appeared in the vertical profiles along the Transect B (Fig. 4B, D and F). The upwelled water was lift to 10 m in the coastal area, and the temperature and salinity were <23 °C and >34, respectively, where there was high Chl *a* (2 mg m^{-3}). The Taiwan Bank upwelling, located on the Taiwan Bank, had high salinity and low temperature with high Chl *a* (up to 2 mg m^{-3}). In contrast, the shelf break was covered by oligotrophic water with very low Chl *a* (0.5 mg m^{-3}).

3.3. Satellite observations

3.3.1. Climatological seasonal variability of SST and chlorophyll a

The climatological seasonal mean satellite AVHRR (1985–2006) SST in the southern Taiwan Strait showed a similar distribution pattern to the field observations (described above), in that a significant difference between the NE monsoon and SW monsoon was observed (Fig. 5). In the NE monsoon season, low temperature and high Chl *a* Zhejiang–Fujian Coastal Current water was found southward along the coast of mainland China. This high Chl *a* area extended from the coastal area to the Taiwan Bank area (Fig. 5A and C). On the other hand, warm oligotrophic Kuroshio Water intruded into the southern Taiwan Strait along the southern shelf margin (Fig. 5A).

During the SW monsoon, the whole Taiwan Strait area was covered by warm and oligotrophic water. However, two high Chl *a* (2 mg m^{-3}) and low temperature (25 °C) upwelled water areas appeared (Fig. 5B and D). Both areas, covered by the high Chl *a* and low SST, were good indicators of upwelling.

3.3.2. Monthly mean SST and chlorophyll a in three typical stations

The seasonal variations of temperature and Chl *a* in three typical stations, which represented two upwelling areas (the Dongshan upwelling and Taiwan Bank upwelling) and the shelf break, are shown in Fig. 6. The monthly mean SST showed similar seasonal patterns at the three stations, with high temperature (28 °C) in summer and low temperature (20 °C) in winter. However, the monthly mean Chl *a* showed a significant difference between these three stations, which might be due to different physical–chemical mechanisms. In coastal station B1, the Chl *a* showed two peaks and large stand deviations, one in July (up to 1.85 ± 1.18 mg m^{-3}) and the other in December (2.03 ± 1.03 mg m^{-3}) and January (2.03 ± 1.43 mg m^{-3}). During the inter-monsoon (September–October, April.–June.), Chl *a* was <1 mg m^{-3}. A comparison of ANOVA results (Table 1) using the LSD method showed that the monthly mean Chl *a* concentration in December–January (NE) and July (SW) were significantly higher than in the other months ($n=117$, $p<0.01$). While a high Chl *a* (in the range 0.6–1.4 mg m^{-3}, with a mean value of 1 mg m^{-3}) was observed in the Taiwan Bank

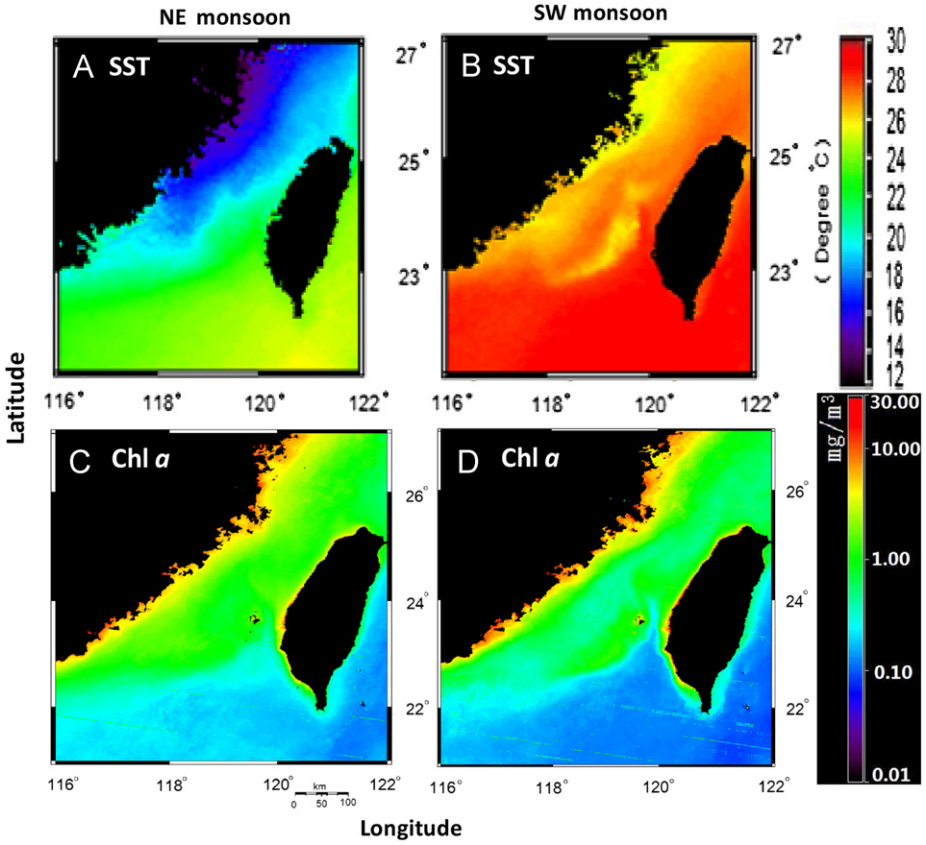

Fig. 5. Climatological seasonal mean sea surface temperature (1985–2006) and sea surface Chl *a* (1997–2007) in the southern Taiwan Strait. (A) SST, NE monsoon, (B) SST, SW monsoon, (C) Chl *a*, NE monsoon and (D) Chl *a*, SW monsoon. The Sea Surface Temperature (SST) was derived from AVHRR from January, 1985 to December, 2006. The surface Chl *a* was derived from SeaWiFS from December, 1997 to December, 2003, and MODIS from January, 2004 to December, 2007, respectively.

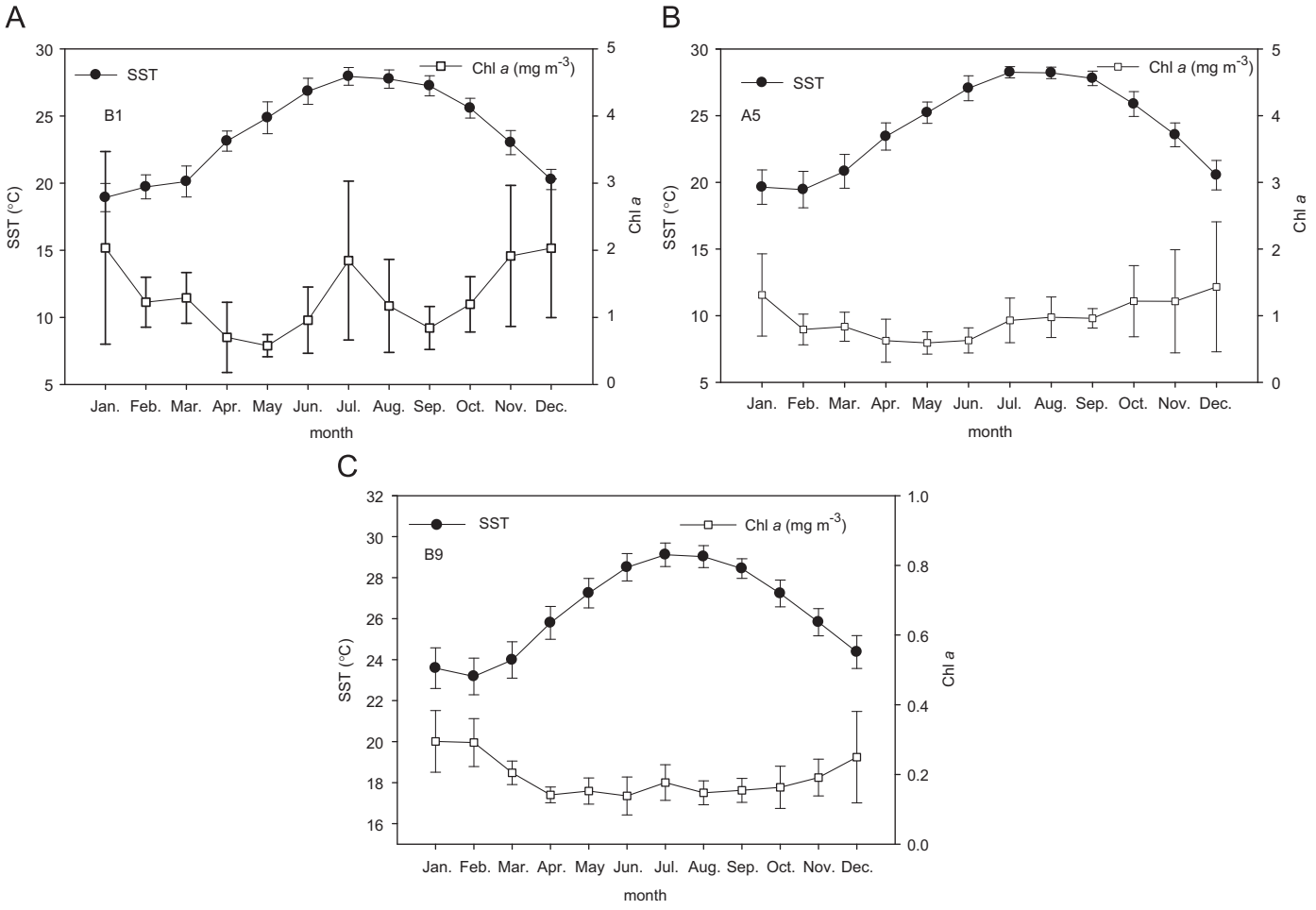

Fig. 6. Monthly mean and standard deviation of Sea Surface Temperature (SST) and chlorophyll *a* concentration (Chl *a*) in the three representative stations (B1, A5 and B9) for the three sub-areas in the southern Taiwan Strait. Data of SST and Chl *a* were from 1985 to 2006 and 1998 to 2007, respectively.

Table 1
ANOVA results of monthly chlorophyll *a* concentration (Chl *a*) in the three representative stations (B1, A5 and B9) for the three sub-areas in the southern Taiwan Strait.

Stations		Sum of squares	df	Mean square	*F*	*p*-value
B9	Between groups	0.312	11	0.028	7.602	0.000**
	Within groups	0.358	96	0.004		
	Total	0.670	107			
B1	Between groups	29.241	11	2.658	4.287	0.000**
	Within groups	65.111	105	0.620		
	Total	94.352	116			
A5	Between groups	8.662	11	0.787	2.822	0.003**
	Within groups	28.739	103	0.279		
	Total	37.401	114			

** $p < 0.01$, very significant difference.

area year-round (Stn. A5). Although, the one-way ANOVA confirmed that Chl *a* also showed significant temporal variations ($n = 115$, $p < 0.01$) in different months, the low values (about 0.6 mg m^{-3}) only occurred in April, May and June when it is the transition of NE to SW monsoon, and also the period with the lowest wind speeds. Besides, in the shelf break area (Stn. B9), the variations of monthly mean Chl *a* concentration showed one peak, and relatively higher Chl *a* (0.3 ± 0.09 mg m^{-3}) was also shown during the NE monsoon season (November–February). A one-way ANOVA and LSD analysis demonstrated significant seasonal variations in the shelf break sub-area of the southern Taiwan Strait ($n = 108$, $p < 0.01$).

4. Discussion

4.1. Temporal variation of Chl a in the southern Taiwan Strait

Compared with the results in the 1987–1988 cruises, Kang (2009) showed contrary results during the 2006–2007 cruises (Fig. 7). Low temperature and rich nutrients coastal current water and strong mixing were observed during the NE monsoon. However, during the SW monsoon, the low temperature and high Chl *a* areas did not occur. In the coastal area, the surface was covered by high temperature (> 28 °C) and low salinity (< 32)

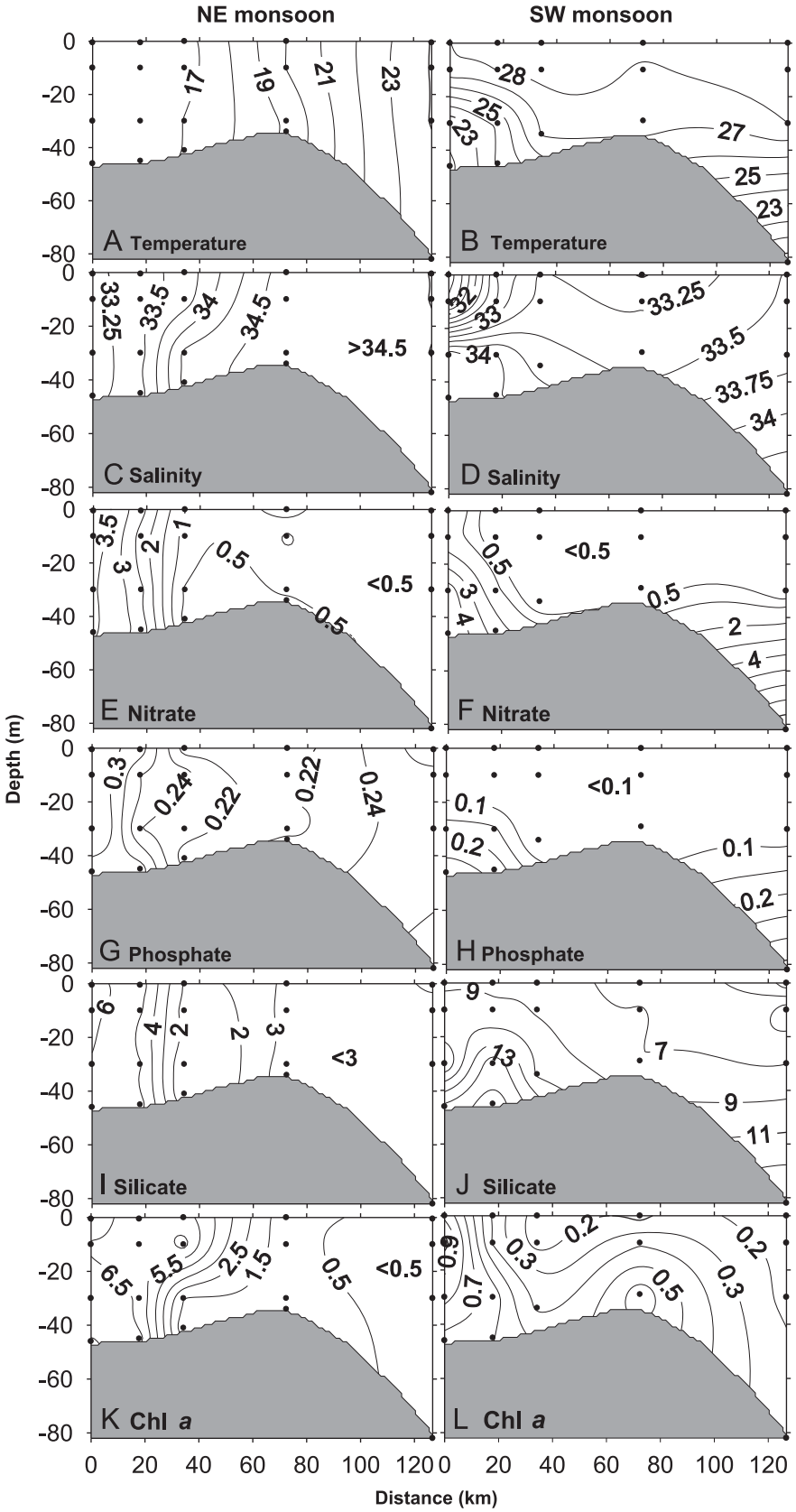

Fig. 7. Variations of temperature (°C), salinity, chlorophyll *a* (mg m^{-3}), nitrate, phosphate and silicate concentration (μmol L^{-1}) along Transect B in the southern Taiwan Strait during the NorthEast (NE) monsoon (left panel) and SouthWest (SW) monsoon (right panel) in August 2006, and February 2007. (redrawn from Kang, 2009).

water, which may be originated from the Pearl River discharge water (Gan et al., 2009b). And also, the low temperature and high salinity water was not observed in the Taiwan Bank area. In addition, both the nitrate and phosphate concentrations in the euphotic zone were lower than 0.5 and 0.1 μmol L^{-1}, respectively. Therefore, the upwelling strength during the SW monsoon

in 2006 cruise was not as strong as the previous studies, whereas the mixing and ZFCC still prevailed during the NE monsoon. Hence, during these cruises, the Chl *a* was higher during the NE monsoon than that during the SW monsoon.

Actually, the explanations of the temporal variations of Chl *a* are complex and cannot be based on a couple of cruises in the southern Taiwan Strait. Some studies report that Chl *a* was higher in the SW monsoon than in the NE monsoon in the Taiwan Strait, due to the upwelling events in the SW monsoon and low temperature and high turbidity in the NE monsoon (Zhang et al., 1997; Zheng et al., 2002; Naik and Chen, 2008). Although, the low temperature may induce temperature limitation, but the temperatures are higher than 16 °C in the study area, and the dominant phytoplankton species, such as *Skeletonema costatum* and *Nitzschia delicatissima*, are eurythermal species. Therefore, temperature would not limit phytoplankton growth during the NE monsoon in the southern Taiwan Strait. Although vertical mixing can also induce light limitation, the euphotic depth in this region is about 20–30 m. Actually, there is always a high Chl *a* front (Chl $a > 1$ mg m^{-3}) coinciding with temperature and nutrients fronts in this area during the NE monsoon. In a normal situation, this front was observed in the Transect A or B in the study area (Fig. 3; Chen and Wang, 2006). Basically, in the north of the front, the low temperature and high turbidity may limit phytoplankton growth, whereas in the south of the front the key may turn to nutrients. However, during an El Niño event, the northeast monsoon is weakened and led to diminished advection of the cold and eutrophic Zhejiang–Fujian Coastal Current, and concomitantly, an expansive intrusion of the warm and oligotrophic South China Sea Warm Current/Kuroshio Branch Water to the Taiwan Strait. Therefore, this front was moved northward. During this winter, the area ratio of the warm water (2 °C above the regional mean) to the cold water (2 °C below the regional mean) in the Taiwan Strait increased by 25%. In addition, field observations confirmed that the mixed layer in the Taiwan Strait became more nutrient-poor and most area was halved by the eutrophic water (Chl $a > 1$ mg m^{-3}) (Shang et al., 2005). During the SW monsoon, the intensity of upwelling is impacted by the wind speed, currents and even ENSO events (Tang et al., 2004; Hong et al., 2009). Shang et al. (2004) reveal that the upwelling in the coastal area is an intermittent event, using satellites and field short-term data. The phytoplankton growth has a time lag of 2 days behind an upwelling event (SW wind and cold area appeared), and the duration of upwelling events in the Taiwan Strait was between 7 and 12 days (Shang et al., 2004). The processes that increased and decreased the integrated mean Chl *a*, from 0.5 to 3 mg m^{-3} and from 4.5 to 1 mg m^{-3}, just only needed 5–7 days, respectively, (Hu, 2009). Therefore, the unstable upwelling process causes the phytoplankton standing stocks to show high temporal variations in the coastal area. Many studies only showed the instant situation regarding the phytoplankton standing stock in coastal areas in the southern Taiwan Strait. Our results also showed high mean Chl *a* and their standard deviations at Stn. B1 (Fig. 6), and some different temporal patterns of Chl *a* between Fig. 4 and 7.

From the long-term satellite data analysis, we acquired more extensive and long-term records of temporal variations of phytoplankton in the southern Taiwan Strait. According to the long-term satellite data (Fig. 8) for the whole study area, mean Chl *a* concentrations during the NE monsoon (0.69 mg m^{-3}) were significantly higher than that during the SW monsoon season (0.53 mg m^{-3}) ($n=10$, $p<0.01$, paired test) (Tables 2 and 3). This significant relationship can also be found in the Taiwan Bank and shelf break areas. However, for the coastal area, this relationship did not exist ($n=10$, $p>0.05$, paired test). Furthermore, as mentioned above, the temporal variation pattern of phytoplankton

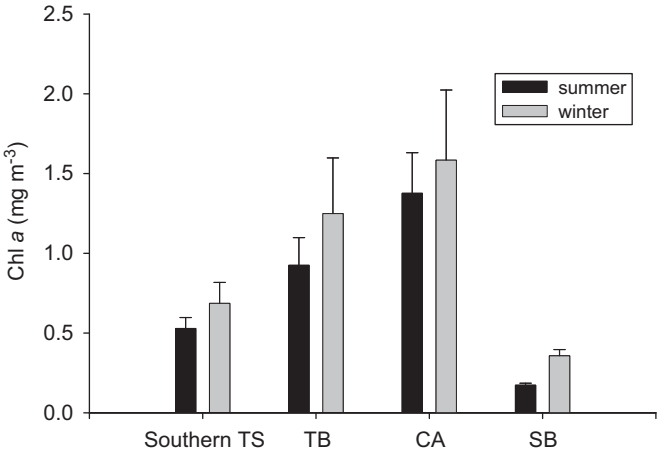

Fig. 8. Mean and standard deviation of chlorophyll *a* concentration of summer and winter in the southern Taiwan Strait derived from satellite data, during 1998–2007. See Fig. 1 and text for definition of the three sub-areas. STS, southern Taiwan Strait; TB, Taiwan Bank; CA, Coastal Area; and SB, shelf break.

Table 2
The satellite mean and Standard Deviation (SD) of chlorophyll *a* concentration (mg m^{-3}) during NE and SW monsoons in the southern Taiwan Strait.

Monsoon	SW monsoon				NE monsoon			
Area	STS	TB	CA	SB	STS	TB	CA	SB
Mean	0.53	0.92	1.38	0.17	0.69	1.25	1.58	0.36
SD	0.068	0.174	0.254	0.012	0.131	0.349	0.440	0.040
n	10	10	10	10	10	10	10	10

STS, Southern Taiwan Strait; TB, Taiwan Bank; CA, Coastal Area; SB, Shelf break.

Table 3
The paired samples test of chlorophyll *a* concentration (mg m^{-3}) between the NE and SW monsoons.

Area	Mean differences	*p*-value
Southern Taiwan Strait	−0.16	0.003*
Taiwan bank	−0.32	0.022**
Coastal area	−0.21	0.174
Shelf break	−0.18	0.000*

* $p<0.01$, very significant difference.
** $p<0.05$, significant difference.

biomass in the coast, Taiwan Bank and outer shelf waters was significantly different (Fig. 6). In the coastal area, two peak types were induced by the NE and SW monsoon, related to coastal current and upwelling, respectively. One peak type, formed in the outer shelf water, resulted from vertical mixing of the NE monsoon. Moreover, a situation of high phytoplankton standing stock which was induced by the nutrient-rich subsurface waters of the Kuroshio always occurred in the Taiwan Bank area. The nutrient-rich subsurface water was lifted as the bottom topography shoaled (Fig. 7F and H).

4.2. Nutrient input between the different monsoons

Under either the upwelling induced by the SW monsoon or coastal current and vertical mixing induced by the NE monsoon, the nutrient supply is affected by wind speed. However, the

mechanisms of nutrient input in the sub-areas during NE and SW monsoons are different.

4.2.1. NE monsoon

The Zhejiang–Fujian Coastal Current and vertical mixing are proposed as the two most important nutrient sources during the NE monsoon. Chen et al. (2006) indicated that an active vertical mixing induced by the NE monsoon occurs throughout the northern South China Sea and the mixed layer depth is much shallower in winter than in other seasons. The nutricline became weaker and sustained an elevated phytoplankton standing stock which resulted in mean Chl *a* (0.65 mg m^{-3}) in winter was 8 times higher than that in summer. We believe that, during the NE monsoon period, the vertical mixing induced by NE monsoon plays an important role in nutrient supply and subsequently induced phytoplankton enhancement in the study area. On the other hand, the Zhejiang–Fujian Coastal Current, characterized by low temperature and nutrient-rich water, has significant impacts on the southern Taiwan Strait during the NE monsoon period (Jan et al., 1998, 2006; Lee et al., 2005). In the coastal area, the nitrate, phosphate and silicate concentrations reached up to 3.5, 0.3 and 6 μmol L^{-1}, respectively, (Fig. 7E, G and I). Although the coastal current can be a major nutrient source in the NE monsoon season, the low temperature, low salinity and nutrient-rich coastal current water can only be observed in coastal area, and the water column showed a homogenous vertical distribution through the transect (Fig. 4A, C and 7A, C). Therefore, it appeared that the vertical mixing induced by the strong NE wind was more important than the coastal current. Furthermore, many studies confirm that the Taiwan Bank upwelling appears to have a year-round complex mechanism including the influence of wind stress, tides, bottom topography and Kuroshio intrusion (Hong et al., 1991; Hu et al., 2003). In addition, many studies confirm that the Kuroshio intrusion was significantly higher during the NE monsoon than the SW monsoon. However, this upwelling phenomena is not clearly shown in the vertical distribution of temperature and salinity during the NE monsoon (Fig. 4 and 7). We believe that this is because of the strong mixing during the NE monsoon, since the salinity of Taiwan Bank and the shelf break area during the NE monsoon reached 34.5, which is much higher than during the SW monsoon (Fig. 4A, C, 7A, C). Therefore, the strong vertical mixing which was induced by the strong NE wind brought up nutrient-rich sub-surface water for phytoplankton growth. Based on the satellite data from 1999 to 2007, a significant relationship between wind speed and Chl *a* existed during the NE monsoon (Fig. 9A, $r^2 = 0.23$, $p < 0.05$). The results demonstrate that both vertical mixing and coastal current are enhanced by the strong NE wind (Jan et al., 1998; Chen et al., 2006; Guan and Fang, 2006). Under these two major processes, the nutrient-rich and high Chl *a* water occupied the entire water column on the shelf, and this situation was also confirmed by the survey results of 2006–2007 (Fig. 7).

4.2.2. SW monsoon

During the SW monsoon season, some studies indicate that nutrient-rich and cold upwelled water usually occurs along the coast of mainland China (e.g. the Dongshan upwelling) and the Taiwan Bank. Both these upwelling events have a close coupling with the SW wind (Tang et al., 2002, 2004; Shang et al., 2004). Fig. 7 reveals that relatively high nitrate, phosphate and silicate concentrations coincide with cold and high salinity upwelled water (Fig. 7F, H and J). In addition, the two high Chl *a* areas are clearly shown in these areas. It is noted that the nitrate and phosphate concentrations are very low in the surface water. Ou et al. (2006) observed that the phytoplankton community suffers from *P* stress even in the upwelling area in the southern Taiwan Strait. Moreover, the phytoplankton's *P*-stress strengthened during the end of the bloom period in the coastal upwelling area. This is one of the reasons why the Chl *a* concentration is not as high as the other upwelling areas.

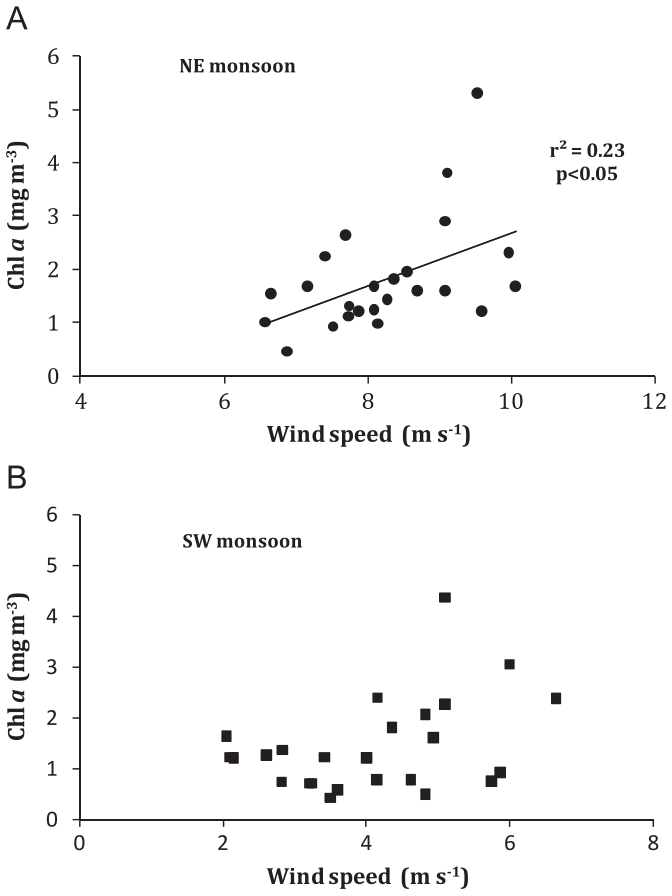

Fig. 9. The correlation between wind speed and chlorophyll *a* concentration during the NorthEast (NE) monsoon (A) and SouthWest (SW) monsoon (B) from 1999 to 2007.

The significant relationship between wind speed and Chl *a* concentration did not exist during the SW monsoon (Fig. 9B). During the SW monsoon, the Dongshan upwelling was principally caused by the cold waters that be derived from the famous "East Guangdong upwelling", which was induced by Ekman transport (Gan et al., 2009a, 2009b). Hence, the Dongshan upwelling should be engendered by the SW monsoon. However, these processes are complicated and unstable (Shang et al., 2004; Gan et al., 2009a). Furthermore, the Taiwan Bank upwelling appears to have a year-round complex mechanism including the influence of wind stress, tide, bottom topography and Kuroshio intrusion (Hong et al., 1991; Hu et al., 2003). Some authors demonstrate that the Kuroshio branch intrudes into the southern Taiwan Strait through the Luzon Strait year-round and there is a close coupling between the Kuroshio intrusion and the Taiwan Bank upwelling (Shaw, 1989, 1991; Jan et al., 1998; Hu et al., 2000). Therefore, the Kuroshio intrusion is identified as more important than the SW wind for the formation of the Taiwan Bank upwelling (Chen et al., 1982; Xiao, 1988; Hu et al., 2003). Our data showed that Chl *a* was always high at Stn. A5 in the Taiwan Bank area throughout the year (Fig. 6B). These values were higher than those in coastal area in the inter-monsoon and shelf break area all year round. Therefore, a weaker relationship between Chl *a* and wind speed was found in the SW monsoon season compared with the NE monsoon season.

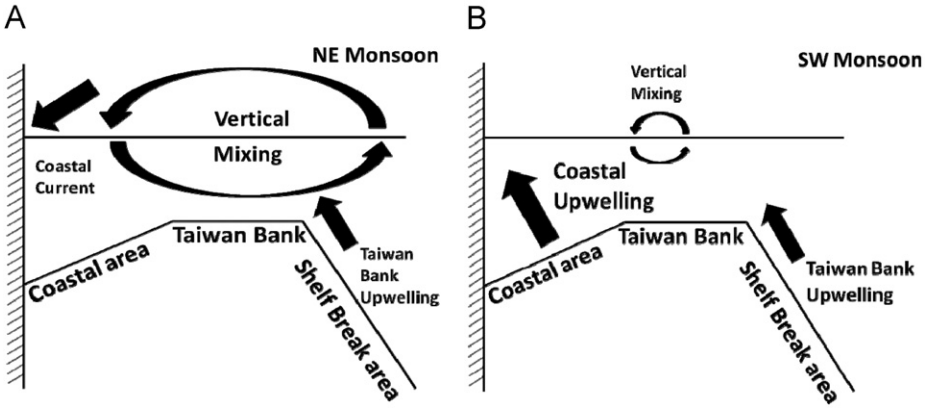

Fig. 10. Schematic diagram on seasonal patterns of the major processes in the southern Taiwan Strait.

5. Conclusions

In conclusion, nutrient availability affects the temporal variation patterns of phytoplankton standing stock in the southern Taiwan Strait. In the euphotic zone, with nutrient input from upwelling, coastal currents and vertical mixing, phytoplankton growth is enhanced. The mechanism of nutrient supply showed a significant difference between the NE and SW monsoons in the southern Taiwan Strait (Fig. 10). During the NE monsoon, nutrients can be brought into the euphotic zone of the study area by upwelling, Zhejiang–Fujian Coastal Current and vertical mixing. The Zhejiang–Fujian Coastal Current water has significant impacts on the coastal area, however, for most areas the vertical mixing is the dominant process enhancing phytoplankton growth during the NE monsoon (Fig. 10A). During the SW monsoon, nutrients were mainly input into the coastal area and Taiwan Bank by the upwelling process (Fig. 10B). Therefore, in the coastal area there were two high phytoplankton standing stocks which occurred during the NE and SW monsoon periods. The Taiwan Bank upwelling resulted from a shallowing of the topography and the Kuroshio intrusion, and exhibited high phytoplankton standing stock all year-round. The shelf break area was similar to the South China Sea, with a high phytoplankton standing stock during the NE monsoon. For the whole study area, there was a significant coupling between Chl *a* and wind speed during the NE monsoon, while it was very weak during the SW monsoon. The mean Chl *a* during the NE monsoon ($0.69\ mg\ m^{-3}$) was significantly higher than that during the SW monsoon ($0.53\ mg\ m^{-3}$) ($p < 0.01$). These results suggested that the East Asia monsoon system could have significant ecological impacts on temporal and spatial variations in phytoplankton biomass.

Acknowledgments

The authors would like to thank the captains and crews of RV ‘‘Dongfanghong 1’’, ‘‘Yanping 1’’ and ‘‘Yanping 2’’, who made concerted efforts during field sampling. We are grateful to Profs. W.Q. Ruan, L.Y. Wu and F. Zhang for their help during the cruise and nutrient data collection. We also thank Prof. John Hodgkiss of The University of Hong Kong for his language editing and comments on the manuscript. This work was supported by the grants of the China NSF (Nos. 40730846, 40706041, and 40925018) and the National Basic Research Program (China GLOBEC-IMERS Program, No. 2006CB400604).

References

Chen, T.A., Wang, S.L., 2006. A salinity front in the southern East China Sea separating the Chinese coastal and Taiwan Strait waters from Kuroshio waters. Continental Shelf Research 26, 1636–1653.

Chen, C.C., Shiah, F.K., Chung, S.W., Liu, K.K., 2006. Winter phytoplankton blooms in the shallow mixed layer of the South China Sea enhanced by upwelling. Journal of Marine Systems 59, 97–110.

Chen, J.Q., Fu, Z.L., Li, F.X., 1982. A study on upwelling in Minnan–Taiwan Shoal fishing ground. Journal of Oceanography in Taiwan Strait 1 (2), 5–13 (in Chinese with English abstract).

Gan, J.P., Cheung, A., Guo, X.G., Li., L., 2009a. Intensified upwelling over a widened shelf in the northeastern South China Sea. Journal of Geophysical Research—Oceans 114, C09019. doi:10.1029/2007JC004660.

Gan, J.P., Li, L., Wang, D.X., Guo, X.G., 2009b. Interaction of a river plume with coastal upwelling in the northeastern South China Sea. Continental Shelf Research 29, 728–740.

Gordon, H.R., Wang, M., 1994. Retrieval of water-leaving radiance and aerosol optical thickness over the oceans with SeaWiFS: A preliminary algorithm. Applied Optics 33, 443–452.

Guan, B.X., Fang, G.H., 2006. Winter counter-wind currents off the southeastern China coast: A review. Journal of Oceanography 62, 1–24.

Hong, H.S., Qiu, S.Y., Ruan, W.Q., Hong, G.C., 1991. Minnan–Taiwan Bank Fishing Ground Upwelling Ecosystem Study. In: Hong, H.S., Qiu, S.Y., Ruan, W.Q., Hong, G.C. (Eds.), Minnan–Taiwan Bank Fishing Ground Upwelling Ecosystem Study. Science Press, Beijing, pp. 1–18 (in Chinese with English abstract).

Hong, H.S., Ruan, W.Q., Huang, B.Q., Wang, H.L., Zhang, F., 1997. Studies on the primary production and its controlling mechanism in the Taiwan Strait. In: Hong, H.S. (Ed.), Oceanography in China (7): Primary Productivity and its Controlling Mechanism in Taiwan Strait Regions. China Ocean Press, Beijing, pp. 1–14 (in Chinese with English abstract).

Hong, H.S., Zhang, C.Y., Shang, S.L., Huang, B.Q., Li, Y.H., Li, X.D., Yu, J.T., 2009. Interannual variability of summer coastal upwelling in the Taiwan Strait. Continental Shelf Research 29, 479–484.

Hu, J.Y., Kawamura, H., Hong, H.S., Qi, Y.Q., 2000. A review on the currents in the South China Sea: Seasonal Circulation, South China Sea Warm Current and Kuroshio Intrusion. Journal of Oceanography 56, 617–624.

Hu, J.Y., Kawamura, H., Hong, H.S., Pan, W.R., 2003. A review of research on the upwelling in the Taiwan Strait. Bulletin of Marine Science 73, 605–628.

Hu, J., 2009. Studies on Phytoplankton Community and Response to Upwelling in the Southern Taiwan Strait. Ph.D Dissertation, Xiamen University (in Chinese with English abstract).

Huang, B.Q., Hong, H.S., Wang, H.L., 1999. Size-fractionated primary productivity and the phytoplankton–bacteria relationship in the Taiwan Strait. Marine Ecology—Progress Series 183, 29–38.

Jan, S., Chern, C.S., Wang, J., 1998. A numerical study of currents in the Taiwan Strait during winter. Terrestrial Atmospheric and Oceanic Sciences 9, 615–632.

Jan, S., Sheu, D.D., Kuo, H.M., 2006. Water mass and throughflow transport variability in the Taiwan Strait. Journal of Geophysical Research 111, C12012. doi:10.1029/2006JC003656.

Jeffrey, S.W., Humphrey, G.F., 1975. New spectrophotometric equations for determining chlorophylls a, b, c_1 and c_2 in higher plants, algae and natural phytoplankton. Biochemistry Physiology Pflanzen 167, 191–194.

Kang J.H., 2009. Studies on seasonal variation of chlorophyll a and primary production on the Taiwan Strait and its adjacent sea area. Master Thesis, Xiamen University (in Chinese with English abstract).

Lee, M.A., Chang, Y., Lee, K.T., Chen, J.W., Liu, D.C., Su, W.C., 2005. A satellite and field view of the winter SST variability in the Taiwan Strait. Proceedings of the IGARSS 2005: IEEE International Geoscience and Remote Sensing Symposium, Vols. 1–8, pp. 2621–2626.

Naik, H., Chen, C.T.A., 2008. Biogeochemical cycling in the Taiwan Strait. Estuarine Coastal and Shelf Science 78, 603–612.

O'Reilly, J.E., Maritorena, S., Siegel, D., O'Brien, M.C., Toole, D., Mitchell, B.G., et al., 2000. Ocean color chlorophyll algorithms for SeaWiFS, OC2, and OC4: Version 4. In: Hooker, S.B., Firestone, E.R. (Eds.), SeaWiFS postlaunch technical report series SeaWiFS postlaunch calibration and validation analyses, part 3, vol. 11. NASA Goddard Space Flight Center, Greenbelt, Maryland, pp. 9–23.

Ou, L.J., Huang, B.Q., Lin, L.Z., Hong, H.S., Zhang, F., Chen, Z.Z., 2006. Phosphorus stress of phytoplankton in the Taiwan Strait determined by bulk and single-cell alkaline phosphatase activity assays. Marine Ecology—Progress Series 327, 95–106.

Pai, S.C., Yang, C.C., Riley, J.P., 1990a. Effects of acidity and molybdate concentration on the kinetics of the formation of the phosphoantimonylmolybdenum blue complex. Analytica Chimica Acta 229, 115–120.

Pai, S.C., Yang, C.C., Riley, J.P., 1990b. Formation kinetics of the pink azo dye in the determination of nitrite in natural water. Analytica Chimica Acta 232, 235–349.

Parsons, T.R., Maita, Y., Lalli, C.M., 1984. A Manual of Chemical and Biological Methods for Seawater Analysis. Pergamon Press, New York, pp. 1–173.

Schott, F.A., McCreary, J.P., 2001. The monsoon circulation of the Indian Ocean. Progress in Oceanography 51, 1–123.

Shang, S.L., Zhang, C.Y., Hong, H.S., Shang, S.P., Chai, F., 2004. Short-term variability of chlorophyll associated with upwelling events in the Taiwan Strait during the southwest monsoon of 1998. Deep-Sea Research Part II 51, 1113–1127.

Shang, S.L., Zhang, C.Y., Hong, H.S., Liu, Q., Wong, G.T.F., Hu, C., Huang, B.Q., 2005. Hydrographic and biological changes in the Taiwan Strait during the 1997–1998 El Nino winter. Geophysical Research Letters, 32. doi:10.1029/2005GL022578.

Shaw, P.T., 1989. The intrusion of water masses into the southwest of Taiwan. Journal of Geophysical Research 94, 18213–18226.

Shaw, P.T., 1991. The seasonal variation of the intrusion of the Philippine Sea water into the South China Sea. Journal of Geophysical Research 96, 821–827.

Tang, D.L., Kawamura, H., Guan, L., 2004. Long-time observation of annual variation of Taiwan Strait upwelling in summer season. Advances in Space Research 33, 307–312.

Tang, D.L., Kester, D.R., Ni, I.H., Kawamura, H., Hong, H.S., 2002. Upwelling in the Taiwan Strait during the summer monsoon detected by satellite and shipboard measurements. Remote Sensing of Environment 83, 457–471.

Wang, D.Z., Hong, H.S., Huang, B.Q., Lin, X.J., 2002. Phytoplankton biomass (chl a) in the Taiwan Strait (1997–1999). Chinese Journal of Oceanology and Limnology 20 (Special Issue), 33–46.

Wan, X.F., Pan, A.J., Guo, X.G., 2007. Seasonal and interannual variability of the chlorophyll concentration in the surface ocean of the Taiwan Strait. Journal of Oceanography in Taiwan Strait 26 (1), 36–45 (in Chinese with English abstract).

Xiao, H., 1988. Studies of coastal upwelling in western Taiwan Strait. Journal of Taiwan Strait 7 China Ocean Press, Beijing, pp. 1–202 (in Chinese with English abstract).

Zhang, C.Y., Hu, C.M., Shang, S.L., Muller-Karger, F.E., Li, Y., Dai, M.H., Huang, B.Q., Ning, X.R., Hong, H.S., 2006a. Bridging between SeaWiFS and MODIS for continuity of chlorophyll—A concentration assessments off Southeastern China. Remote Sensing of Environment 102, 250–263.

Zhang, C.Y., 2006b. Response of chlorophyll a concentrations to multi-scale environmental variations in the Taiwan Strait. Ph.D Dissertation, Xiamen University (in Chinese with English abstract).

Zhang, F., Yang, Y., Huang, B.Q., 1997. Effect of physical input of nutrients on the chlorophyll a content in the Taiwan Strait. In: Hong, H.S. (Ed.), Oceanography in China (7): Primary Productivity and its Controlling mechanism in Taiwan Strait Regions. China Ocean Press, Beijing, pp. 1–14 (in Chinese with English abstract).

Zheng, T.L., Hong, H.S., Wang, F., Maskaoui, K., Su, J.Q., Tian, Y., 2002. The distribution characteristics of bacterial beta-glucosidase activity in Taiwan Strait. Marine Pollution Bulletin 45, 168–176.